Phys. Status Solidi B **247**, Nos. 11–12, 2915–2919 (2010) / **DOI** 10.1002/pssb.201000818

physica status solidi b
www.pss-b.com
basic solid state physics

Growth and properties of chemically modified graphene

Hye Jin Park*[,1], Viera Skákalová[1,2], Jannik Meyer[3], Dong Su Lee[1], Takayuki Iwasaki[1], Chris Bumby[4], Ute Kaiser[3], and Siegmar Roth[5]

[1] Max Planck Institute for Solid State Research, Heisenbergstraße 1, 70569 Stuttgart, Germany
[2] Danubia Nanotech s.r.o., Ilkovičova 3, 84104 Bratislava, Slovakia
[3] Electron Microscopy Group of Materials Science, University of Ulm, Albert Einstein Allee 11, 89069 Ulm, Germany
[4] The MacDiarmid Institute for Advanced Materials and Nanotechnology, Victoria University of Wellington, New Zealand
[5] School of Electrical Engineering, Korea University, Seoul 136-713, South Korea

Received 11 August 2010, revised 25 August 2010, accepted 27 August 2010
Published online 4 October 2010

Keywords chemical structure, chemical vapour deposition, graphene, nitrogen substituted graphene

* Corresponding author: e-mail h.park@fkf.mpg.de, Fax: +49 711 689 1010

Chemically modified graphene was synthesized by chemical vapour deposition (CVD) with ammonia gas introduced during the CVD process. The use of two different metal catalyst films [nickel (Ni) or copper (Cu)] results in distinctly different forms of structural defects in the honeycomb lattice of graphene under identical synthesis conditions. The Ni catalyst film gave rise to numerous "flower-like" defects, where carbon atoms formed core hexagons surrounded by pentagons alternated with heptagons, whilst graphene grown on a Cu catalyst film contained a much higher concentration of substituted nitrogen atoms. The samples were characterized by a variety of spectroscopic and microscopic methods complemented with electrical transport measurements.

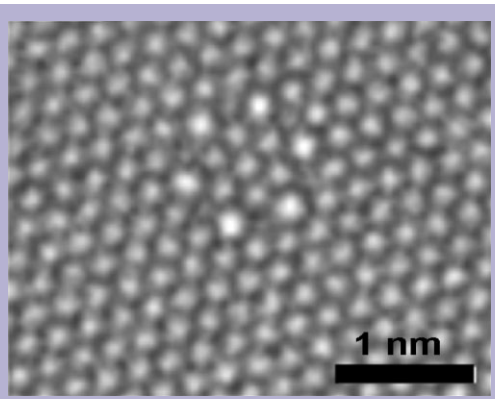

1 Introduction The discovery of single layer graphene and its fascinating properties [1] has ensured that the development of new methods [2–5] to produce large area graphene of high quality has become a hot issue. Recently, Bae et al. [4] have prepared a 30 square inch graphene sheet using the chemical vapour deposition (CVD) method. This has demonstrated the potential of the CVD method to produce large area single- or few-layer graphene (FLG) sheets suitable for industrial applications. The structural properties of the products obtained from a CVD graphene synthesis are determined by several tunable parameters, including: composition of the incoming gas feedstock, choice of the metal catalyst, reaction time and the cooling rate. Previous work has demonstrated the CVD synthesis of substitutionally doped graphene in order to obtain either n- or p-type semiconductors [6], or to produce metal free electrocatalysts [7]. This is achieved through the introduction into the feedstock flow of doping precursors containing either nitrogen or boron. Nitrogen-doped graphene has also been produced by the carbon arc discharge method; using graphite in a nitrogen atmosphere [8, 9]; and by annealing graphene or graphene oxide with ammonia [10] or under nitrogen plasma [11]. However, the chemical structure of the modified graphene obtained in these cases was often not determined clearly. Besides a certain content of nitrogen atoms identified by elemental analysis and/or spectroscopic methods, the product usually contains unspecified structural defects in the hexagonal lattice.

Previously [12], we have reported on CVD-grown FLG produced in our laboratory and on its structural and physical properties. In this report, we present our results on the synthesis and characterization of nitrogen-modified FLG

(N_FLG). CVD synthesis was undertaken using two different metal catalyst substrates, nickel (Ni) and copper (Cu). In both cases methane and ammonia were chosen as the carbon and nitrogen sources. High-resolution transmission electron microscopy (HR-TEM) has revealed substantially different effects of the Ni and Cu substrates on the growth of nitrogen-modified graphene. Using the Ni substrate, we found numerous 'flower-like' lattice defects, where carbon atoms formed core hexagons surrounded by alternating pentagons and heptagons, whereas the N_FLG grown on the Cu substrate contained much higher concentrations of substituted nitrogen atoms. Besides HR-TEM the samples were characterized by a variety of spectroscopic and microscopic methods. Electrical transport measurements showed that, despite a significant decrease in its electrical conductivity, our N-doped FLG does not exhibit a semiconductor-like energy gap in its electronic structure but instead clearly shows a metallic character, where, when cooling towards 4 K, its conductivity saturates at a constant non-zero value. (In this study, we refer to the nitrogen modified FLG sheet on $Ni/SiO_2/Si$ as a N_FLG_Ni and the nitrogen modified FLG sheet on $Cu/SiO_2/Si$ as a N_FLG_Cu. Graphene means a single layer domain from the FLG sheet).

2 Experiments

2.1 Synthesis Nitrogen modified FLG (N_FLG) was prepared by CVD following the procedure [12] applied for the growth of a pristine FLG sheet, with modifications described below. Nickel (Ni, 300 nm) and copper (Cu, 400 nm) films deposited by electron beam evaporator on SiO_2/Si substrates ($2 \times 2\,cm^2$) were used as catalysts. The Ni- (or Cu-) coated substrate was located in the middle of a quartz tube under a flow of argon (200 sccm) and hydrogen (200 sccm) and heated to 1000 °C with a heating rate of 40 °C/min. The substrate was then further annealed at 1000 °C for 20 min before a mixture of gases with a composition ($CH_4/Ar/H_2 = 50{:}200{:}2000$ sccm) was introduced at 980 °C for 3 min (or 10 min). The sample was then cooled at a steady rate of ca. 6.7 °C/min. During cooling, ammonia was substituted for the CH_4 flow within the temperature range 700–300 °C. Introducing ammonia at lower temperatures than the carbon deposition was necessary because, at high temperature, ammonia would react corrosively with the metal substrate, causing damage to the catalyst layer. The sample was then further cooled to room temperature under Ar (200 sccm) and H_2 (500 sccm) flow.

2.2 Transfer onto arbitrary substrates To enable HR-TEM and electrical transport studies it was necessary to transfer the as-grown N_FLG onto arbitrary substrates (in our case either a silicon substrate or a TEM grid). This was achieved in the following manner: poly(bisphenol A carbonate) (PC) was dissolved in chloroform to produce a 15 wt.% solution. The PC/chloroform solution was deposited onto the as-grown N_FLG_Ni substrate by spin-coating at 500 rpm for 2 min. The deposited PC formed a homogeneous film with a thickness of ~10 μm. The N_FLG/PC film was released as a free-stranding film by chemical etching of the metal catalyst layer with a $FeCl_3$ (1 M) solution, followed by treatment with a concentrated HCl solution for 30 min. The etching time in the $FeCl_3$ (1 M) solution was about 6 h. Following etching, the N_FLG/PC film was rinsed several times with DI-water and dried with dry nitrogen gas. It was then placed onto a silicon substrate or TEM grid, and the PC was removed by dissolution in chloroform. In order to further remove any remaining adsorbed organic contaminants, the transferred N-FLG film and new substrate were heated in air to 200 °C for 10 min.

2.3 Characterization Raman scattering measurements were performed by an NT-MDT confocal spectrometer at room temperature using the 488 nm excitation. The X-ray photoelectron spectroscopy (XPS) spectra were taken by a hemispherical analyzer using a monochromatized AlKα X-ray source. Scanning electron microscopy (SEM) analysis was carried out with a high-resolution FEI XL30 SFGE analytical SEM operated at 0.8 kV. TEM was performed using an imaging-side spherical-aberration-corrected Titan 80-300 (FEI, Netherlands), operated at 80 kV. The detection of nitrogen atoms within the N_FLG lattice will be reported separately [13].

The temperature dependence of the electrical conductivity of nitrogen-modified graphene in the N_FLG was investigated by a 4-probe measurement method. For this purpose, a domain of single layer graphene on SiO_2 (300 nm thick)/Si was identified by optical microscopy contrast [14] and a Hall-bar geometry was defined by means of electron beam lithography and oxygen plasma etching. The selected region of single-layer graphene was protected from the oxygen plasma by evaporated aluminium while the remainder of the sample was exposed to oxygen plasma and removed. The oxidized aluminium was then removed with KOH solution (1 M) and rinsed and dried repeatedly. Finally a Cr/Au electrode system was deposited onto the Hall-bar shaped sample using electron beam lithography. A Keithley 2400 source-meter providing a constant current of 1 μA was connected to the outer electrodes and the voltage drop between the inner electrodes was recorded with a Keithley 2000 voltmeter. The channel length of the inner pair of electrodes was 2.5 μm. Before measurement the sample was placed into the sample chamber and annealed at 393 K for 24 h under vacuum (10^{-7} mbar) and then the chamber was filled with He gas. The conductance of the sample was measured as a function of temperature from 300 K down to 4 K.

3 Results and discussion

To summarize, the CVD process for growth of FLG includes three steps. The first step is an annealing process that activates the catalyst film with hydrogen at 1000 °C for 20 min. The second step is the CVD reaction itself during which methane (CH_4) is introduced and catalytically decomposed at the catalyst surface so depositing carbon atoms. The third step is a cooling process whereby, under non-equilibrium conditions, carbon

dissolved within the catalyst layer precipitates at the surface and then segregates as additional layers of carbon are formed. The cooling rate has a crucial influence on the number of layers of the FLG as well as on its crystallinity.

The differing effect of the Ni versus Cu catalyst on the formation of the FLG layers is well-known. It has previously been reported that, due to the low carbon solubility in Cu, fewer graphene layers grow during the Cu-assisted CVD process [15]. According to Ref. [16], carbon solubility at 1000 °C and 1 atm in Cu is only 0.028 at.%, whilst in Ni the solubility reaches 1 at.%. Therefore, to reach the critical dissolved carbon concentration for a continuous FLG sheet over the substrate, CVD growth on a Cu substrate requires a longer reaction time (10 min) than for the Ni substrate (3 min).

When ammonia was introduced into the reactor at 1000 °C together with methane, no graphene was obtained. Reactive species such as hydrogen or activated ammonium ion produced during the decomposition of ammonia reacted vigorously with the metal film, thus destroying the smooth surface of the catalyst which is necessary for the growth of a continuous graphene sheet. Figure 1(a) shows the modified morphology of the originally smooth Ni surface after the CVD process with ammonia. Micron-sized crystal grains were etched from the Ni film by the reactive products of the decomposed ammonia. Instead of producing two-dimensional FLG, the Ni grains served as seeds for the growth of quasi-one dimensional carbon nanotubes [Fig. 1(b)]. A different result was obtained when ammonia was introduced at a lower temperature after the CVD-reaction with methane was finished. This was done during cooling between 700 and 300 °C. Comparison of the SEM images of the surface morphologies after cooling of the Ni polycrystalline substrate [Fig. 1(c)] and the Cu polycrystalline substrate [Fig. 1(d)] indicate some differences. The sample grown on Cu film shows less contrast near the grain boundaries, whilst the sample grown on the Ni film shows dark contrast at the grain boundaries. This indicates that more graphitic layers are formed between the crystalline Ni grains due to carbon segregation.

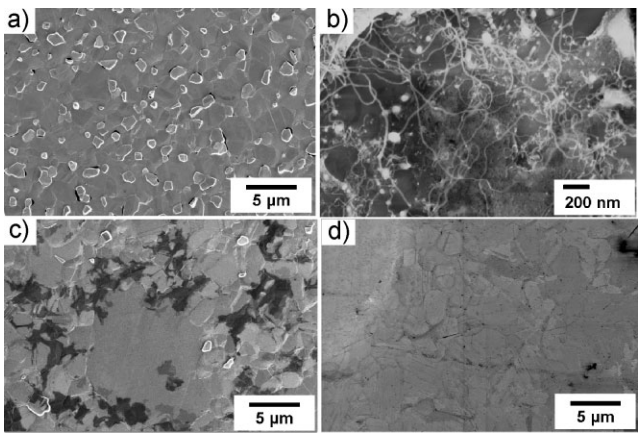

Figure 1 SEM images of (a) the Ni film etched by ammonia at 1000 °C, (b) carbon nanotubes grown from the etched Ni grain, (c) N_FLG on Ni substrate and (d) N_FLG on Cu substrate when ammonia was introduces only during cooling.

The CVD grown N_FGL upon the metal catalyst film was transferred to a SiO_2/Si substrate with an oxide layer of 300 nm. Figure 2(a, c) shows optical images of the transferred N_FGL. Gold markers separated by a distance of 80 μm give the scale. The transferred N_FGL_Ni appears rather inhomogeneous.

Dark deposits of thick carbon (more than five graphitic layers) decorate the Ni grain boundaries. In different regions of the brighter areas, a variable number of graphitic layers is observed [Fig. 2(a)].

The transferred N_FGL_Cu is composed of thinner and more homogeneous layers consistent with the results for pristine FLG grown on a Cu substrate, as reported [15]. There are three modes of Raman spectra, which provide information on the number of graphitic layers and on the crystallinity of graphene. Using a laser excitation wavelength of 514.5 nm, their positions in pristine graphene are as follows; the D mode at about 1350 cm^{-1}, the G mode at 1582 cm^{-1} and the 2D mode at about 2700 cm^{-1} [17]. The G and 2D modes exhibit changes in their shape, position and relative intensities with variation of the number of graphene layers, defects, strain, substrates and doping level [18, 21]. In the case of our N_FLG samples, the Raman spectrum of a single layer N_FLG_Ni shows a high intensity of the D mode (~1352 cm^{-1}) due to a disorder in the crystalline structure. However, the 2D-mode intensity (~2696 cm^{-1}) still remains relatively high. A slight shift of the G-mode located at 1587 cm^{-1} indicates doping. The Raman spectrum of the N_FLG_Cu with the G-mode at 1583 cm^{-1}, D-mode at 1357 cm^{-1} and 2D mode at 2704 cm^{-1} does not differ significantly from that of pristine graphene. In order to probe

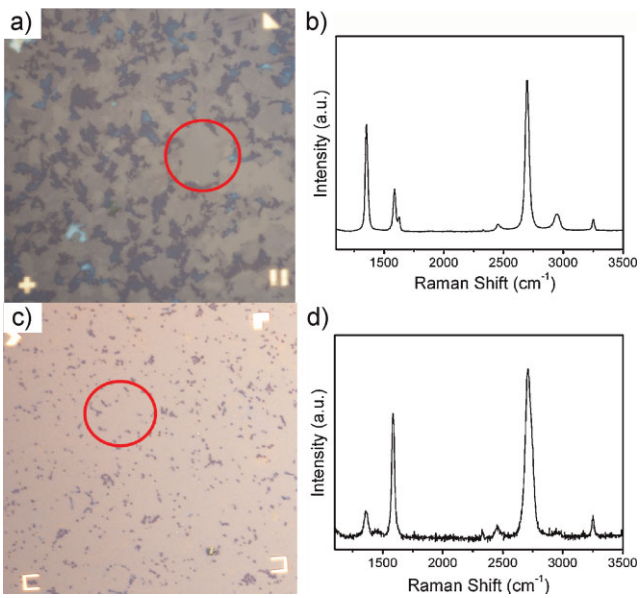

Figure 2 (online colour at: www.pss-b.com) Optical images of transferred FLG sheets from Ni (a) and Cu (c) and Raman spectrum of CVD grown graphene on Ni (b) and Cu (d).

the concentration of the nitrogen atoms, XPS was employed. XPS analysis showed a very low content of nitrogen (∼0.01 at.%) in the N_FLG_Ni sample, whereas in the N_FLG_Cu sample, the concentration of nitrogen reached up to 0.6 at.%, varying with the position across the sample. As such, although precise control of the homogeneity and level of nitrogen doping remains a challenge, the Cu catalyst was found to be more efficient for substitutional doping of graphene by nitrogen.

We assume that Cu might play an important role in introducing nitrogen atoms into the hexagonal structure of graphene, possibly through a coordination bond between Cu and nitrogen. An HR-TEM image in Fig. 3(b) shows N substitution atoms in a graphene sheet. The contrast of the dark spots is mainly due to a change in the electronic configuration around the N-atoms, and will be described in detail elsewhere (Meyer et al., to be published). The N concentration in the Cu grown samples as estimated from HR-TEM observations is ca. 0.1 at.%. Figure 3(a) shows a single-layer graphene domain from N_FLG_Ni where a dominant feature is the appearance of flower-like structural defects. Most of them contain a core of seven hexagons tilted by 90° with respect to the basic hexagonal structure, surrounded by six pentagons alternated with six heptagons. This defect was only observed in nitrogen-modified graphene samples which had been subjected to ammonia during the cooling stage of the CVD synthesis. Although the flower-like defect formation was initiated when ammonia was introduced, the presence of nitrogen atoms within this flower-like defect has not been proven. The single-atom substitution of carbon by a nitrogen atom was also found only very occasionally, which is in a good agreement with the XPS analysis showing that less than 0.01 at.% of nitrogen was bound in the structure of N_FLG_Ni sample.

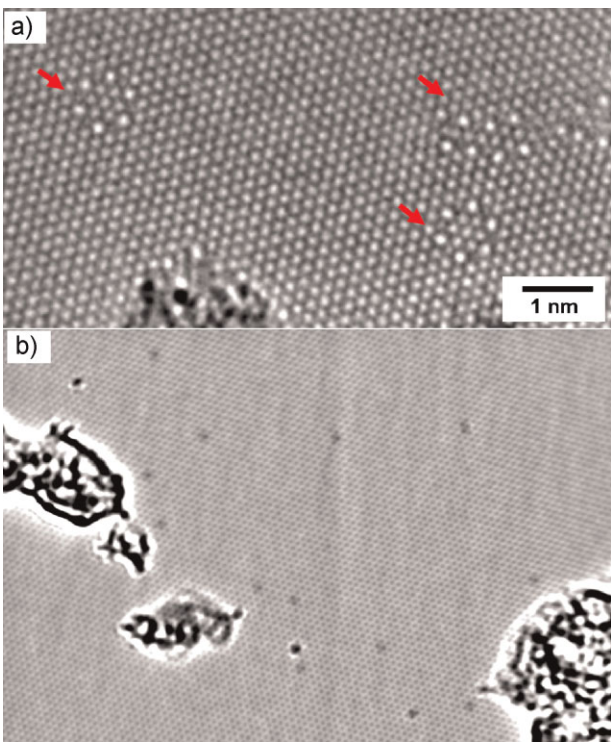

Figure 3 (online colour at: www.pss-b.com) HR-TEM images of modified graphene from Ni substrate (a) and from Cu substrate (b).

The electrical transport properties of single-layer nitrogen-modified graphene Hall-bar devices fabricated from our N_FLG_Ni sample were studied as a function of temperature. We did not observe the opening of a semiconductor gap in our material as has previously been reported in Ref. [6]. We attribute this to the relatively low n-doping of our samples.

Nevertheless, the modified graphene showed interesting temperature dependent behaviour. Figure 4A presents the temperature dependence of the graphene sheet conductance normalized to the value at 300 K. The log–log plot shows data from three samples: a large-area of about 1 mm^2 pristine FLG sheet, a graphene domain selected from this pristine FLG and a modified graphene domain selected from N_FLG_Ni, both in the Hall-bar configuration. The large-area pristine FLG sheet is highly inhomogeneous and the number of graphitic layers contributing to conductance varied across the sample. This sample manifests a highly metallic character with only a moderate increase of conductance by ∼20% as temperature increases from 4.2 to 300 K (Fig. 4A: curve 1). A small single layer graphene domain was selected from this pristine FLG and then a device was fabricated using electron beam lithography. The temperature dependence of the sheet conductance of this device showed a similar, but larger, increase by ∼55% with increasing temperature (Fig. 4A: curve 2). Such a temperature dependence differs from the curves reported for the samples of exfoliated graphene from HOPG via micro-mechanical cleavage method [19, 20], where conductance often decreases with rising temperature showing metallic behaviour affected by scattering on high-energy phonons. This implies that, unlike exfoliated material, thermal effects play an important role in the conductivity of our CVD graphene devices. Single-layer graphene grown by the CVD method consists of several covalently connected crystalline domains [12]. The domain boundaries form energy barriers between the domains and limit delocalization of charge carriers along the sample. As a consequence of this lower crystallinity when compared to exfoliated HOPG, the metallic conduction mechanism is restricted and the effect of thermal assistance at charge transport dominates the observed changes in conductivity as temperature increases.

A similar device was fabricated upon a region of single-layer modified graphene from N_FLG_Ni, by the same procedure as the pristine graphene device. The main features of the temperature dependence of the modified graphene are again quite similar to those of the pristine graphene, but when compared to the previous curve it shows a much stronger increase, by ∼85% of the initial sheet conductance as temperature rises from 50 to 300 K (Fig. 4A: curve 3). However, at low temperatures below 50 K, the conductance

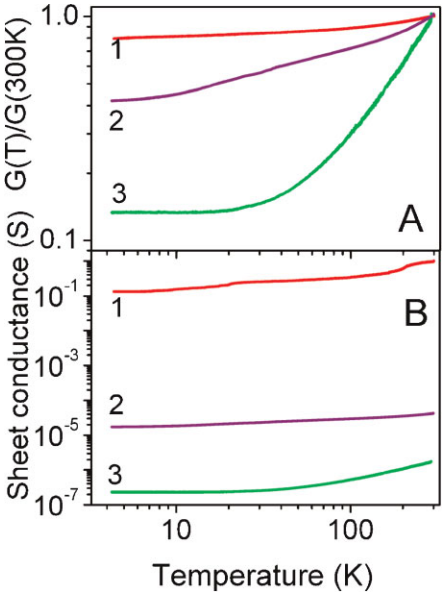

Figure 4 (online colour at: www.pss-b.com) Temperature dependence of (A) normalized sheet conductance to the value at 300 K and of (B) absolute value sheet conductance of three samples: (1) large area (1 mm^2) FLG, (2) a monolayer Hall-bar structured and (3) N-doped monolayer Hall-bar structured graphene, plotted in the log–log scale.

saturates to a constant non-zero value. We expect the defective crystal structure of the modified graphene to contain a large number of localized states in the electronic structure. This would lead to a thermally activated hopping transport of the charge carriers between localized states and this effect will dominate the observed changes in conductivity as the temperature rises to room temperature. However, below 50 K, the temperature-independent conductivity shows metallic behaviour. This could be explained if the metallic regions of graphene form a percolating metallic network that dominates the charge transport at low temperatures where the thermally activated hopping current becomes negligibly small. The electrical transport study of graphene from N_FLG_Cu is ongoing work in our group. The absolute values of sheet conductance for the same three samples are presented in Fig. 4B. The pristine single-layer graphene domain conductance is four orders of magnitude less than that observed for the large-area FLG. The introduction of nitrogen into the structure of graphene causes the observed sheet conductance to drop by a further two orders of magnitude. This is consistent with our interpretation of the relative effects of structural disorder within each sample.

In conclusion, we have synthesized chemically nitrogen-modified graphene by CVD methods using methane and ammonia as carbon and nitrogen sources. The nitrogen-modified graphene grown on a Ni substrate contains unique structural flower-like defects but only a small concentration of nitrogen (0.01 at.%). Much more efficient doping by nitrogen was achieved when Cu was used as the catalyst. The modified N_FLG_Cu shows concentration of up to 0.6 at.% of graphitic nitrogen according to XPS (only 0.1 at.% according to HR-TEM). We show partial results of electrical measurements of the modified graphene sample and other experiments are still ongoing work.

Acknowledgements V. S. acknowledges the Center of Excellence CENAMOST (Slovak Research and Development Agency Contract No. VVCE-0049–07) for support of project APVV-0628-06. S. R. acknowledges support by the World Class University (WCU, R32-2008-000-10082-0) Project of the Korean Ministry of Education, Science and Technology. T. I. acknowledges the JSPS Postdoctoral Fellowship for Research Abroad.

References

[1] A. K. Geim and K. S. Novoselov, Nature Mater. **6**, 183 (2007).
[2] A. Reina, X. Jia, J. Ho, D. Nezich, H. Son, V. Bulovic, M. S. Dresselhaus, and J. Kong, Nano Lett. **9**, 30 (2008).
[3] J. H. Lee, D. W. Shin, V. G. Makotchenko, A. S. Nazarov, V. E. Fedorov, Y. H. Kim, J. Y. Choi, J. M. Kim, and J. B. Yoo, Adv. Mater. **21**, 4383 (2009).
[4] S. Bae, H. Kim, Y. Lee, X. Xu, J.-S. Park, Y. Zheng, J. Balakrishnan, T. Lei, H. Ri Kim, Y. I. Song, Y.-J. Kim, K. S. Kim, B. Ozyilmaz, J.-H. Ahn, B. H. Hong, and S. Iijima, Nature Nanotechnol. **5**, 574 (2010).
[5] X. Li, Y. Zhu, W. Cai, M. Borysiak, B. Han, D. Chen, R. D. Piner, L. Colombo, and R. S. Ruoff, Nano Lett. **9**, 4359 (2009).
[6] D. Wei, Y. Liu, Y. Wang, H. Zhang, L. Huang, and G. Yu, Nano Lett. **9**, 1752 (2009).
[7] L. Qu, Y. Liu, J.-B. Baek, and L. Dai, ACS Nano **4**, 1321 (2010).
[8] P. Sutter, J. T. Sadowski, and E. Sutter, Phys. Rev. B **80**, 245411 (2009).
[9] L. S. Panchakarla, K. S. Subrahmanyam, S. K. Saha, A. Govindaraj, H. R. Krishnamurthy, U. V. Waghmare, and C. N. R. Rao, Adv. Mater. **21**, 4726 (2009).
[10] X. Wang, X. Li, L. Zhang, Y. Yoon, P. K. Weber, H. Wang, J. Guo, and H. Dai, Science **324**, 768 (2009).
[11] X. Li, H. Wang, J. T. Robinson, H. Sanchez, G. Diankov, and H. Dai, J. Am. Chem. Soc. **131**, 15939 (2009).
[12] H. J. Park, J. Meyer, S. Roth, and V. Skákalová, Carbon **48**, 1088 (2010).
[13] J. C. Meyer, S. Kurasch, H. J. Park, V. Skákalová, D. Künzel, A. Groß, A. Chuvilin, G. Algara-Siller, S. Roth, T. Iwasaki, U. Starke, J. Smet, U. Kaiser, arXiv:1006.0712v2 (2010).
[14] I. Jung, M. Pelton, R. Piner, D. A. Dikin, S. Stankovich, S. Watcharotone, M. Hausner, and R. S. Ruoff, Nano Lett. **7**, 3569 (2007).
[15] X. Li, W. Cai, L. Colombo, and R. S. Ruoff, Nano Lett. **9**, 4268 (2009).
[16] T. B. Massalski, Binary Alloy Phase Diagrams, Vol. 1, second ed. (ASM International, USA, 1990).
[17] A. C. Ferrari, Solid State Commun. **143**, 47 (2007).
[18] L. M. Malard, M. A. Pimenta, G. Dresselhaus, and M. S. Dresselhaus, Phys. Rep. **473**, 51 (2009).
[19] Y.-W. Tan, Y. Zhang, H. L. Stormer, and P. Kim, Eur. Phys. J. **148**, 15 (2007).
[20] V. Skákalová, A. B. Kaiser, J. S. Yoo, D. Obergfell, and S. Roth, Phys. Rev. B **80**, 153404 (2009).
[21] C. Casiraghi, Phys. Status Solidi RRL **3**, 175 (2009).